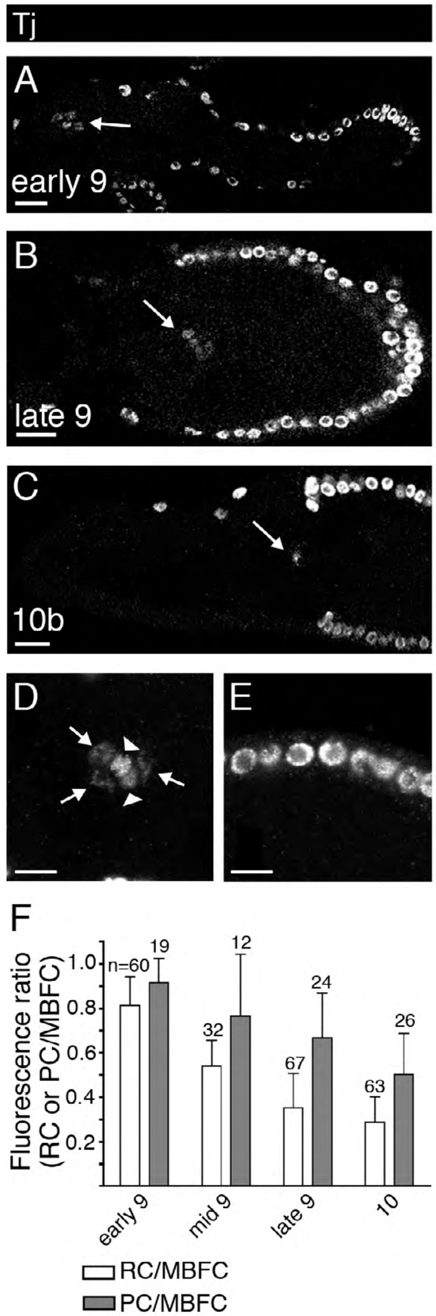


**Fig. S1. Tj expression decreases in the BCC during migration.** (**A-E**) Cryosections confirm the decrease of Tj expression during BCC migration. The long arrows arrows point to the BCC in A-C, the short arrows point to rosette cells and the arrowheads point to polar cells in D. Tj signal is considerably weaker in BCCs (A-D) than in MBFCs (A-C,E) throughout and after migration. (D) Tj expression appears weaker in rosette than in polar cells. Cryosections 15 µm thick were generated using a Leica CM3050S cryostat. (**F**) Measurement of Tj signal intensity shows a gradual decrease of Tj in both rosette and polar cells compared with MBFCs. The graph shows mean + s.d. Each sample size (*n*) represents equal numbers of rosette or polar cells and MBFCs. Scale bars: 20 µm in A-C; 10 µm in D,E. PC, polar cells; RC, rosette cells.

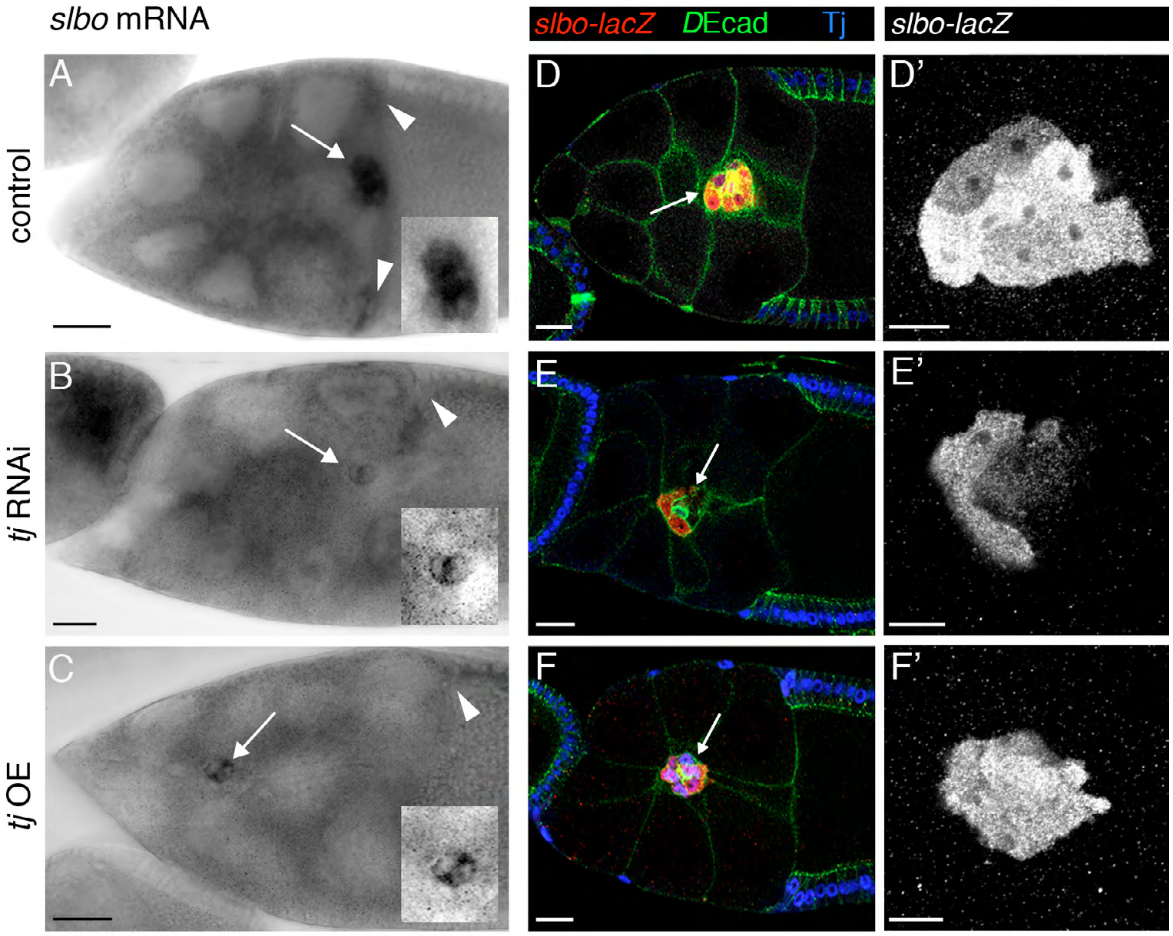


**Fig. S2. Tj reduction or overexpression causes reduction of *slbo* mRNA, but only Tj reduction affects *slbo-lacZ* activity.** (A-F) Stage 10 follicles. (**A-C**) *slbo* mRNA expression in BCCs (arrows, magnified and contrast-enhanced in insets) and centripetal cells (arrowheads). In comparison to the control follicle, where *slbo* mRNA is found in rosette, polar, and centripetal cells (A), *slbo* mRNA is only detected in polar cells, but not in rosette or centripetal cells in follicles with *tj* RNAi (B) or *tj* overexpression (OE) (C). (**D-F′**) *slbo* enhancer (*slbo-lacZ*) activity in BCCs (arrows; magnified in D′-F′). Although *slbo-lacZ* expression varies from cell to cell, compared to the control BCC (D), *slbo* enhancer expression appears reduced in BCCs with *tj* RNAi (E), but remains unchanged in BCCs with *tj* OE (F). Scale bars: 25 µm in A-C; 20 µm in D-F; 10 µm in D′-F′.

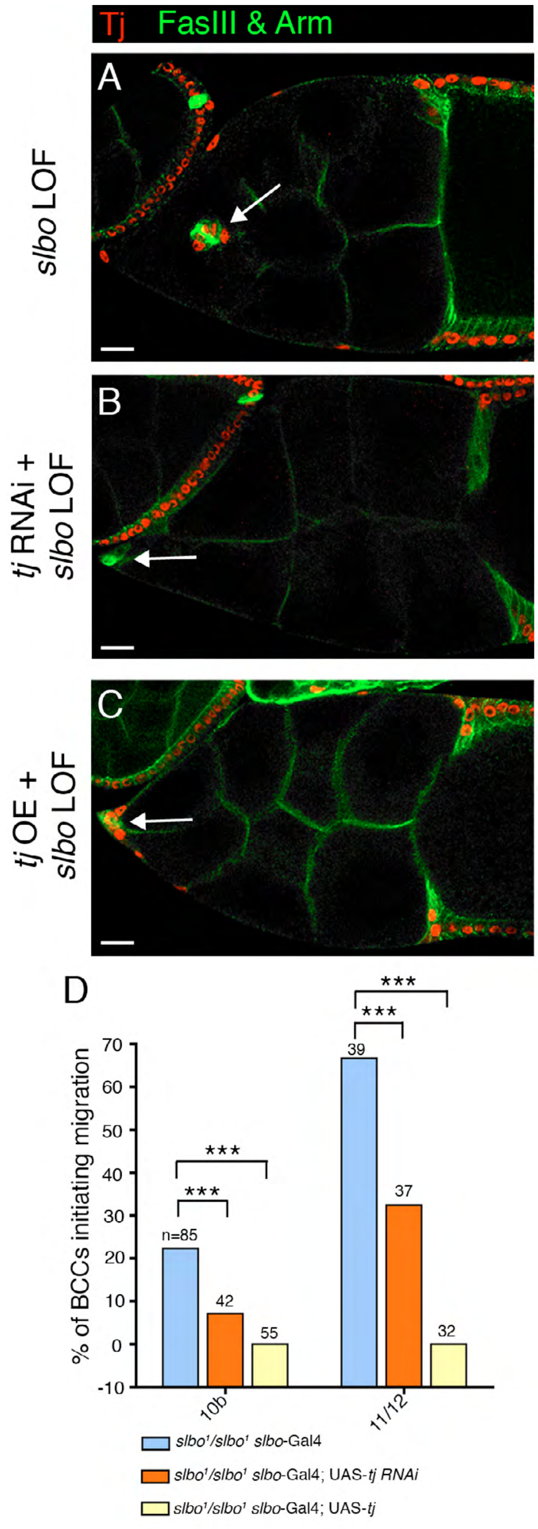


**Fig. S3. Tj reduction or overexpression enhances the BCC migration defect of *slbo*[1] mutants.** (**A-C**) Late stage 10b follicles. Arrows points to BCCs. A *slbo*[1] mutant BCC initiated migration (A). *slbo*[1] mutant BCCs expressing *tj*-RNAi (B) or overexpressing Tj (C) failed to migrate. Note lack of Tj in B and strong Tj signal in C. (**D**) Quantification of the ability of BCCs to initiate migration in response to altered Tj expression in *slbo*[1] mutant BCCs at indicated stages. The graph shows mean + s.d.; *n*, number of BCCs evaluated. ***$P$<0.001. Scale bars: 20 µm.

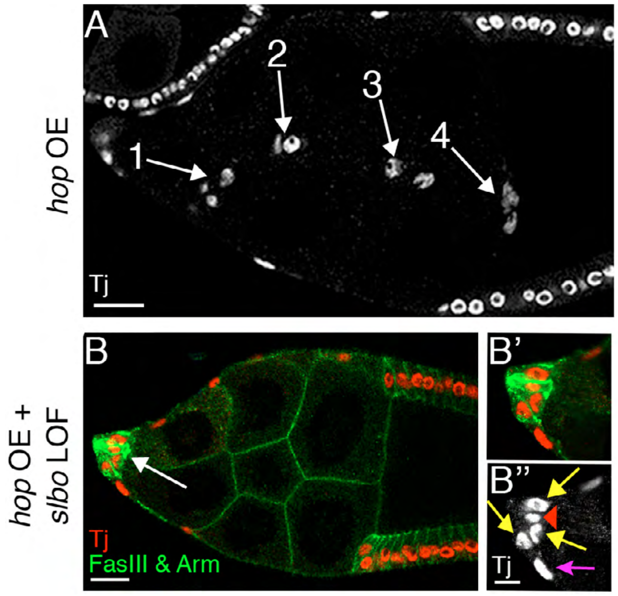


**Fig. S4. The Jak/Stat pathway mediates Tj reduction in the BCC through Slbo.** (**A**) In a Slbo-positive background, ectopic expression of Hop in anterior follicle cells (*c306-Gal4*/+; *UAS-hop3*/+) induces formation of extra migratory rosette cells (1-3), each of which has a reduced Tj level similar to the main BCC (4). (**B-B″**) By contrast, in a *slbo*$^{1}$ mutant background, Tj signal in the BCC (B, arrow; magnified in B′,B″) does not appear reduced in rosette cells (yellow arrows) compared to polar (red arrowhead) and anterior follicle cells (pink arrow) even with Hop overexpression (*slbo*$^{1}$/*slbo*$^{1}$ *slbo-Gal4*; *UAS-hop3*/+). Scale bars: 20 µm in A,B; 10 µm in B′,B″.

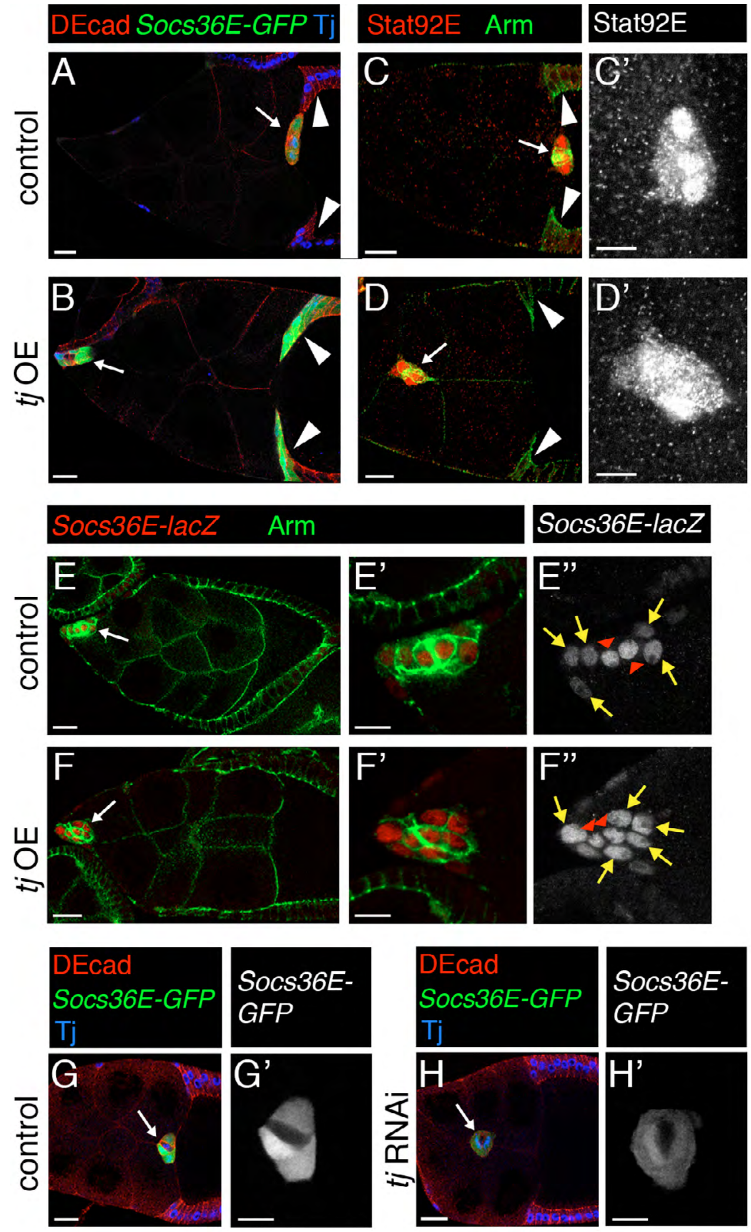


**Fig. S5. Tj enhances expression of *Socs36E*, but not Stat92E.** (A-H′) White arrows point to BCCs in stage 10 follicles (A-D,G-H) and in mid stage 9 follicles (E-F). (**A**,**B**) *Socs36E-GFP* expression is considerably stronger in the BCC and centripetal cells of a *tj*-overexpressing follicle (B) than the control (A). (**C-D′**) Stat92E expression appears similar in control (C,C′) and *tj*-overexpressing BCCs (D,D′). (**E-F″**) In contrast to the control, where polar cells (red arrowheads) show higher *Socs36E-lacZ* (*Socs36E*$^{PZ1647}$) expression than rosette cells (yellow arrows) (E-E″), Tj-overexpressing rosette cells express *Socs36E-lacZ* at a level comparable to polar cells (F-F″). (**G-H′**) *Socs36E-GFP* signal is considerably weaker in a BCC, in which Tj had been knocked down before BCC formation (*c306-Gal4*/+; *Socs36E-GFP*/+; *UAS-tj*$^{RNAi}$/+) (H,H′), than in a control BCC (*c306-Gal4/+; Socs36E-GFP/+*) (G,G′). Scale bars: 20 µm in A-H; 10 µm in C′-H′.